Dai *et al. Applied Biological Chemistry* (2022) 65:56
https://doi.org/10.1186/s13765-022-00723-9

KSABC
The Korean Society for Applied Biological Chemistry

ARTICLE Open Access

circTUBGCP5 promotes liver cancer progression and glycolysis by up-regulating the expression of ACSL4

Wei Dai[1*], Yanqun Duan[2], Wenkang Yuan[1] and Siyu Wang[1]

Abstract

A large number of researches have shown that circular RNA (circRNA) is new hope for the diagnosis or treatment of tumors, including liver cancer (LCa). However, it remains largely unclear the role of circRNA in the progression of LCa and its molecular mechanism. GSE164803 microarray dataset was applied to identify dysregulated circRNAs in LCa and noncancerous tissues. CircTUBGCP5 (hsa_circ_0034049) was selected for further research. Biological functions of circTUBGCP5 were investigated by EdU, colony formation, flow cytometry, glucose consumption and lactate production assay, and in vivo tumorigenesis. RNA pull-down assay and dual-luciferase reporter assay were used to investigate the interaction between circTUBGCP5, miR-144-3p, and ACSL4. We demonstrated that circTUBGCP5 was significantly up-regulated in LCa tissues and cells. CircTUBGCP5 promoted LCa cell proliferation, anti-apoptotic ability, glycolysis, and tumorigenesis at least partially by sponging miR-144-3p to regulate ACSL4 protein level. In conclusion, circTUBGCP5 is a forceful contributor to malignant behaviors and glycolysis of LCa via modulating the circTUBGCP5/miR-144-3p/ACSL4 axis, which has provided a target for the diagnosis and treatment of LCa patients.

Keywords: Liver cancer, circTUBGCP5, miR-144-3p, ACSL4

Introduction

In 2020, worldwide liver cancer (LCa) new cases accounted for 4.6% of the total incidence, and worldwide LCa deaths accounted for 8.3% of the total deaths [1]. Although the treatment strategy for LCa has been continuously perfected, the prognosis of most patients is still unsatisfactory due to its unlimited proliferation and abnormal metabolism [2–4]. Therefore, an in-depth study of the molecular mechanism of LCa progression is essential to find new strategies.

The rapid development of molecular biology research and genome-wide sequencing technology provides abundant resources for the development of biomarkers for better early diagnosis, prognosis prediction, and treatment of LCa [5, 6]. CircRNA is defined as a new type of non-coding RNA molecule with a covalently linked closed-loop structure, which expression is more stable and not easy to degrade by RNA exonuclease [7]. Previous studies have implicated that abnormally expressed circRNA was closely associated with proliferation, apoptosis, metastasis, and aerobic glycolysis of tumor cells by serving as sponges for microRNA (miRNA), RNA-binding protein (RBP) adsorbers, protein/peptide translation templates, regulating transcript alternative splicing [8–11]. For instance, circSLIT2 contributed to pancreatic ductal adenocarcinoma cell aerobic glycolysis and proliferation via sponging miR-510-5p to boost the expression of c-myc [12]. CircRNF13 could suppress the glycolytic process, proliferation, and metastasis by stabilizing SUMO2 protein level and enhancing GLUT1 degradation in nasopharyngeal carcinoma [13]. Moreover, circRHOBTB3 could hamper colorectal cancer cell

*Correspondence: dw20080606@126.com

[1] Hepatopancreatobiliary Surgery, The First Affiliated Hospital of Anhui Medical University, No.218 Jixi Road, Hefei 230022, Anhui, People's Republic of China
Full list of author information is available at the end of the article

Springer Open

© The Author(s) 2022. **Open Access** This article is licensed under a Creative Commons Attribution 4.0 International License, which permits use, sharing, adaptation, distribution and reproduction in any medium or format, as long as you give appropriate credit to the original author(s) and the source, provide a link to the Creative Commons licence, and indicate if changes were made. The images or other third party material in this article are included in the article's Creative Commons licence, unless indicated otherwise in a credit line to the material. If material is not included in the article's Creative Commons licence and your intended use is not permitted by statutory regulation or exceeds the permitted use, you will need to obtain permission directly from the copyright holder. To view a copy of this licence, visit http://creativecommons.org/licenses/by/4.0/.

metastasis through binding to HuR protein and degrading the PTBP1 level [14]. While the effects of circRNA have been extensively disclosed, the exact roles and mechanisms of circRNA in the development of LCa remain unclear.

Cell metabolic reprogramming is considered one of the principal characteristics of cancer, which is beneficial to tumor malignant proliferation and adaptation to unfavorable environments [15, 16]. Regardless of oxygen abundance, tumor cells prefer to depend on glycolysis, which could gain a higher ability to decompose glucose into lactic acid to produce ATP, as the main source of energy metabolism [17]. Prior studies have implicated that changes in tumor microenvironment stress and genes, such as c-myc, could regulate glycolysis-related transporters and enzymes [18, 19]. Aerobic glycolysis has been proved to play a significant role in LCa proliferation, growth, metastasis, and drug resistance [2]. The mechanism of aerobic glycolysis has not been fully elucidated in LCa. Therefore, effective targeted therapy of the LCa cell glycolysis pathway and its upstream regulators may provide a new strategy for LCa therapy.

Here, we screened a novel circRNA circTUBGCP5 (hsa_circ_0034049) which was notably up-regulated in tumor tissues of LCa in the GSE164803 dataset. Then, we evaluated whether circTUBGCP5 could facilitate LCa cell proliferation, anti-apoptotic ability, glycolysis, and tumorigenesis by the miR-144-3p/ACSL4 axis, hoping that our results may aid in identifying a new biomarker for diagnosis and treatment of LCa.

Materials and methods

Human samples

LCa tumor tissues and adjacent normal tissues were taken from forty-six LCa patients who underwent surgery. The inclusion and exclusion criteria of LCa patients were: (1) confirmed pathologic diagnosis of LCa, (2) not receiving preoperative chemotherapy or radiotherapy, and extrahepatic metastases, (3) no previous treatment for LCa, (4) with complete clinical information, (5) randomly selected tissues samples. The excised tissue was immediately frozen in liquid nitrogen and stored at − 80 °C. All experimental procedures were approved by the Ethics Committee of the First Affiliated Hospital of Anhui Medical University. Each patient received written informed consent.

Cell culture and transfection

The human LCa cells Huh-7 (GDC0134; China Center for Type Culture Collection; CCTCC, Wuhan, China) and HCCLM3 (GDC0289; CCTCC) were cultured in DMEM medium (01-056-1A; Bioind, Israel) and RPMI-1640 medium (01-100-1A; Bioind) at 37 °C with 5% CO_2. Human Liver Epithelial-2 cells THLE-2 (T0015001; AddexBio, San Diego, CA, USA) and Human Embryonic Kidney Cells 293 T (T0011002; AddexBio) were maintained in DMEM medium (01-056-1A; Bioind) at 37 °C with 5% CO_2. All medium was added with 1 × penicillin/streptomycin (C0222; Beyotime, Shanghai, China) and 10% FBS (04-001-1A; Bioind).

The pLKO.1-puro-sh-circTUBGCP5 vector (sh-circTUBGCP5) containing shRNA targeting circTUBGCP5 junction sites was constructed by Biofeng (Shanghai, China), followed by packaging into the lentivirus by co-transfecting with psPAX2 and pMD2G into 293 T cells, and infection into Huh-7 and HCCLM3 cells. The miR-144-3p mimic (miR-144-3p), miR-144-3p inhibitor (anti-miR-144-3p), the pcDNA-ACSL4 vector containing full-length ACSL4, pmiR-RB-Report™ luciferase vector (circTUBGCP5-wt, circTUBGCP5-mut, ACSL4-3′ UTR-wt, ACSL4-3′ UTR-mut) containing wild type (wt) and mutated (mut) circTUBGCP5 or ACSL4-3′ UTR sequence were obtained from RiboBio (Guangzhou, China), followed by transfecting into Huh-7 and HCCLM3 cells with Lipofectamine 3000 (L3000008; Invitrogen, Carlsbad, CA, USA).

Quantitative real-time polymerase chain reaction (qRT–PCR) analysis

Trizol (R0016; Beyotime) was employed to extract RNA that then was transcribed into cDNA using miRNA First Strand cDNA Synthesis Kit (B532453; Songon, Shanghai, China) and Universal RT-PCR Kit (RP1100; Solarbio, Beijing, China). ChamQ SYBR qPCR Master Mix (Q311-02; Vazyme, Nanjing, China) was implemented to measure the level of circTUBGCP5, miR-1278, miR-1245-5p, miR-144-3p, and ACSL4 mRNA. U6 was used as the internal reference of miR-1278, miR-1245-5p, and miR-144-3p, while β-actin was employed as the internal reference of circTUBGCP5, and ACSL4 mRNA. The relative expression level was calculated via the $2^{-\Delta\Delta CT}$ method. The primer sequences were synthesized from Songon:

CircTUBGCP5 (Forward 5′-TAACTGTCTCGTCCG TCCTG-3′, Reverse 5′-CAGCCTTGCCATGTCCATTA-3′); ACSL4 (Forward 5′-CATCCCTGGAGCAGATACTCT-3′, Reverse 5′-TCACTTAGGATTTCCCTGGTCC-3′); miR-1278 (Forward 5′-CTCCGAGTAGTACTGTGCATA-3′, Reverse 5′-CTCAACTGGTGTCGTGGAG-3′); miR-144-3p (Forward 5′-GGATTCCGAGTACAGTATAGATGA-3′, Reverse 5′-TCAACTGGTGTCGTGGAGT-3′); miR-145-5p (Forward 5′-ATTCCGAGGTCCAGTTTTCCCA-3′, Reverse 5′-CTCAACTGGTGTCGTGGAGTC-3′); U6 (Forward 5′-CTTCGGCAGCACATATACT-3′,Reverse 5′-AAA ATATGGAACGCTTCACG-3′); β-actin (Forward 5′-CTT CGCGGGCGACGAT-3′ Reverse 5′-CCACATAGGAAT CCTTCTGACC-3′).

Western blot assay

Mammalian protein extraction kit (C600589; Songon) and BCA Protein Quantification Kit (E112-01; Vazyme) were performed to extract total protein and quantitate protein. SDS-PAGE (P0012A; Beyotime) was used to separate proteins of different molecular weight sizes that then were electrotransferred onto the PVDF membranes (F019531; Songon). Subsequently, the membrane was blocked with 5% Nonfat-Dried Milk (P0216; Beyotime) and incubated with primary antibodies c-myc (Anti-c-Myc; ab32072; 1:1000; Abcam), GLUT1 (Anti-Glucose Transporter GLUT1; ab14683; 1:2000; Abcam), ACSL4 (Anti-FACL4; ab155282; 1:20,000; Abcam), and β-actin (beta Actin Antibody; MA5-15,739; 1:5000; Invitrogen) overnight at 4 °C, followed by incubated with Goat Anti-rabbit IgG/HRP antibody (SE134 1:2000; Solarbio) at room temperature for 2 h. ECL Western Blotting Substrate (PE0010; Solarbio) and Image-Pro Plus software were used for the protein of visualization and quantification.

Immunohistochemistry (IHC) assay

Like the previous study [20], tumor samples were fixed, embedded in paraffin, cut into 5 μm thick sections, and incubated with antibodies c-myc (ab32072; 1:100; Abcam), GLUT1 (ab14683; 1:200; Abcam), ACSL4 (Anti-FACL4; ab155282; 1:200; Abcam), followed by IHC Detection Kit (E-IR-R213; Elabscience, Wuhan, China).

Nuclear/cytoplasmic fractionation

Nuclear and cytoplasmic RNAs in Huh-7 and HCCLM3 cells were isolated using PARIS™ Kit (AM1921; Invitrogen). DNA-free™ DNase (AM1906; Invitrogen) was allowed to remove trace amounts of DNA in the nuclear RNA sample. The level of circTUBGCP5, β-actin, and U6 was estimated by qRT–PCR.

RNase R treatment

Huh-7 and HCCLM3 cells RNA (20 μg) was processed with 4U RNase R (M1228-500; Biovision, Milpitas, CA, USA) at 37 °C for 2 h. The level of circTUBGCP5 and β-actin were explored using qRT–PCR.

Cell proliferation assay

Ethynyl-2′-deoxyuridine (EdU) assay: Cells (2×10^5/well) were inoculated in 24-well plates until the normal growth stage. After being treated with EdU Cell Proliferation Kit (E607204; Songon), cells were fixed with 4% paraformaldehyde and incubated with Hoechst 33,342 to stain cell nuclei. Colony formation assay: Cells (500/well) were cultured in 24-well plates for 14 days. 4% Paraformaldehyde Fix Solution (E672002; Songon), 0.2% crystal violet (A600331; Songon), and Image-Pro Plus software were implemented to fix, stain, and quantify the colony.

Cell apoptosis assay

Cells (2×10^5) were collected and stained with Annexin V-fluorescein isothiocyanate (FITC) and propidium iodide (PI) via Annexin V-FITC/PI Detection Kit (E606336; Songon), followed by analysis with flow cytometry.

Caspase-3 and Caspase-9 activity assay

Cells (1×10^6) were collected and processed with Caspase-3 Activity Detection Kit (BC3830; Solarbio) and Caspase-9 Activity Detection Kit (BC3890; Solarbio) to test the hydrolytic activity of Caspase-3 and Caspase-9, which was monitored by microplate reader at wavelength OD405. All values were normalized to cell numbers.

Glucose consumption and lactate production assay

Cells (1×10^6) were collected and dealt with with Glucose Uptake Assay Kit (ab136955; Abcam) and L-Lactate Assay Kit (ab65331; Abcam), followed by measuring output at wavelength OD412 and OD450 with a microplate reader (Invitrogen). All values were normalized to cell numbers.

RNA pull-down assay

The biotin-labeled probe against the circTUBGCP5 junction site (Songon) was incubated with cell lysates, and then Streptavidin immunomagnetic beads (D110557; Songon) were used to pull down biotin-coupled complexes. The circTUBGCP5 bound miR-1278, miR-1245-5p, and miR-144-3p were quantified by qRT–PCR.

Dual-luciferase reporter assay

Luciferase vectors and miR-144-3p were co-transfected into Huh-7 and HCCLM3 cells with Lipofectamine 3000 (L3000008; Invitrogen) for 48 h, followed luciferase activity was assessed via Dual-Lucy Assay Kit (D0010; Solarbio).

Animal experiments

Huh-7 cells (2×10^6) of circTUBGCP5 knockdown were resuspended in 100 μL PBS and then subcutaneously injected into the back of male BALB/cA-nu Mice (HFK, Beijing, China). The length and width of the tumor were assessed with a caliper every 4 days starting on day 3 and the tumor volume was calculated as $(\text{length} \times \text{width}^2 \times 0.5)$. After 27 days, the mice were sacrificed, followed by qRT–PCR, western blot, and IHC to assess the level of circTUBGCP5, ACSL4, c-myc, and GLUT1 in tumor samples. The animal experiments were

permitted by the Animal Care and Use Committee of the First Affiliated Hospital of Anhui Medical University.

Statistical analysis

GraphPad Prism 9 was used to analyze the values that were shown as means ± standard deviations (SD). Student's *t*-test or one-way ANOVA with Tukey's post hoc test respectively were employed for comparisons between two or more groups. $P < 0.05$ was considered statistically significant.

Results

CircTUBGCP5 was overexpressed in LCa tissues and cells.

Dataset GSE164803 in the GEO datasets, which contained 6 pairs of HCC tissue as well as noncancerous tissues, was applied to identify dysregulated circRNAs in LCa. We found there are 96 up-regulated circRNAs and 156 down-regulated circRNAs ($|\mathrm{Log_2}(\text{fold change})| \geq 1$; adj.P.Value < 0.05) in LCa by analyzing GSE164803 microarray datasets with the GEO2R tool (Fig. 1A). Among them, the expression of circTUBGCP5 showed one of the most dramatic changes in LCa tissues (Fig. 1B). Next, we measured the expression level of circTUBGCP5 was significantly increasing in LCa tissues and cells (Huh-7 and HCCLM3) than normal tissues and cells (THLE-2) by qRT–PCR (Fig. 1C, D). The structure of circTUBGCP5 was illustrated by circPrimer2.0 [21], which showed circTUBGCP5 derived from exons 2–8 of the TUBGCP5 gene (Genomic location: chr15:22,835,915–22,846,952 +, circBase ID: hsa_circ_0034049), and back-splicing junction sites of circTUBGCP5 were proved using Sanger sequencing (Fig. 1E). To further characterize circTUBGCP5, the cytoplasmic/nuclear isolation experiment was employed to illustrate the location of circTUBGCP5, which indicated that most of the circTUBGCP5 could be found in the cytoplasm of Huh-7 and HCCLM3 cells (Fig. 1F, G). Furthermore, compared with β-actin mRNA, circTUBGCP5 was resistant to RNAse R treatment, and implicating circTUBGCP5 was circular (Fig. 1H, I). These data demonstrated that circTUBGCP5 was overexpressed in LCa tissues and cells, implying its potential to be related to LCa progress.

CircTUBGCP5 enhanced LCa cell proliferation, anti-apoptotic ability, and glycolysis

To explore the function of circTUBGCP5 in LCa, shRNA targeting the back spliced site of circTUBGCP5 was utilized to knock down circTUBGCP5 expression. In comparison with the pLKO.1-puro-sh-NC (sh-NC) group, the level of circTUBGCP5 was efficiently lower about fivefold in the sh-circTUBGCP5 group (Fig. 2A). circTUBGCP5 downregulation strikingly restrained Huh-7 and HCCLM3 cell proliferation (Fig. 2B, C), and contributed to cell apoptosis (Fig. 2D). Moreover, circTUBGCP5 knockdown triggered the augment of Caspase-3 and Caspase-9 activity (Fig. 2E, F). To examine the effect of circTUBGCP5 on glycolysis in LCa, we examined glucose consumption and lactate production of LCa cells. The results showed that glucose uptake and lactate production were conspicuously reduced when circTUBGCP5 was knocked down in Huh-7 and HCCLM3 cells (Fig. 2G, H). Given the promoting role of c-myc and GLUT1 on glycolysis in LCa[18, 19], we detected the protein level of c-myc and GLUT1. Knockdown of circTUBGCP5 suppressed the level of c-myc and GLUT1 via western blot in Huh-7 and HCCLM3 cells (Fig. 2I, J). Taken together, these findings indicated that circTUBGCP5 could enhance LCa cell proliferation, anti-apoptotic ability, and glycolysis.

CircTUBGCP5 directly interacted with miR-144-3p in LCa cells

To figure out the molecular mechanism of circTUBGCP5 in LCa, the starbase (https://starbase.sysu.edu.cn), [22] circbank (http://www.circbank.cn/index.html), [23] and circinteractome (https://circinteractome.nia.nih.gov) [24] database were utilized to predict the potential miRNAs of circTUBGCP5. Venn diagrams showed that 3 miRNAs (miR-278, miR-145-5p, and miR-144-3p) consistently had binding sites to circTUBGCP5 in the three databases (Fig. 3A). Furthermore, RNA pull-down and qRT–PCR assay showed that the amount of miR-144-3p was pulled down by circTUBGCP5, indicating circTUBGCP5 could bind with miR-144-3p (Fig. 3B, C). The complementary base sequences between positions 180–188 of circTUBGCP5 and miR-144-3p were shown in Fig. 3D. To test if miR-144-3p binds with circTUBGCP5 in LCa, miR-144-3p mimic (miR-144-3p) was introduced into Huh-7 and HCCLM3 cells. qRT–PCR data presented that the level of miR-144-3p was notably increased in Huh-7 and HCCLM3 cells after transfecting with miR-144-3p (Fig. 3E). Moreover, the Luciferase reporter assay showed that miR-144-3p prominently reduced the luciferase activity of circTUBGCP5-wt but not circTUBGCP5-mut (Fig. 2F, G). Next, down-regulated miR-144-3p was validated by qRT–PCR in LCa tissues and cells (Fig. 3H, I). These results demonstrated that circTUBGCP5 may act as a sponge for miR-144-3p in LCa.

MiR-144-3p targeted ACSL4 in LCa cells

To disclose the precise mechanism underlying the function of circTUBGCP5, the downstream targets of miR-144-3p were investigated. miRDB (http://mirdb.org/) [25] and Targetscan (http://www.targetscan.org/vert_72/) [26] were analyzed to predict the potential miR-144-3p-target genes. The GEPIA database (http://

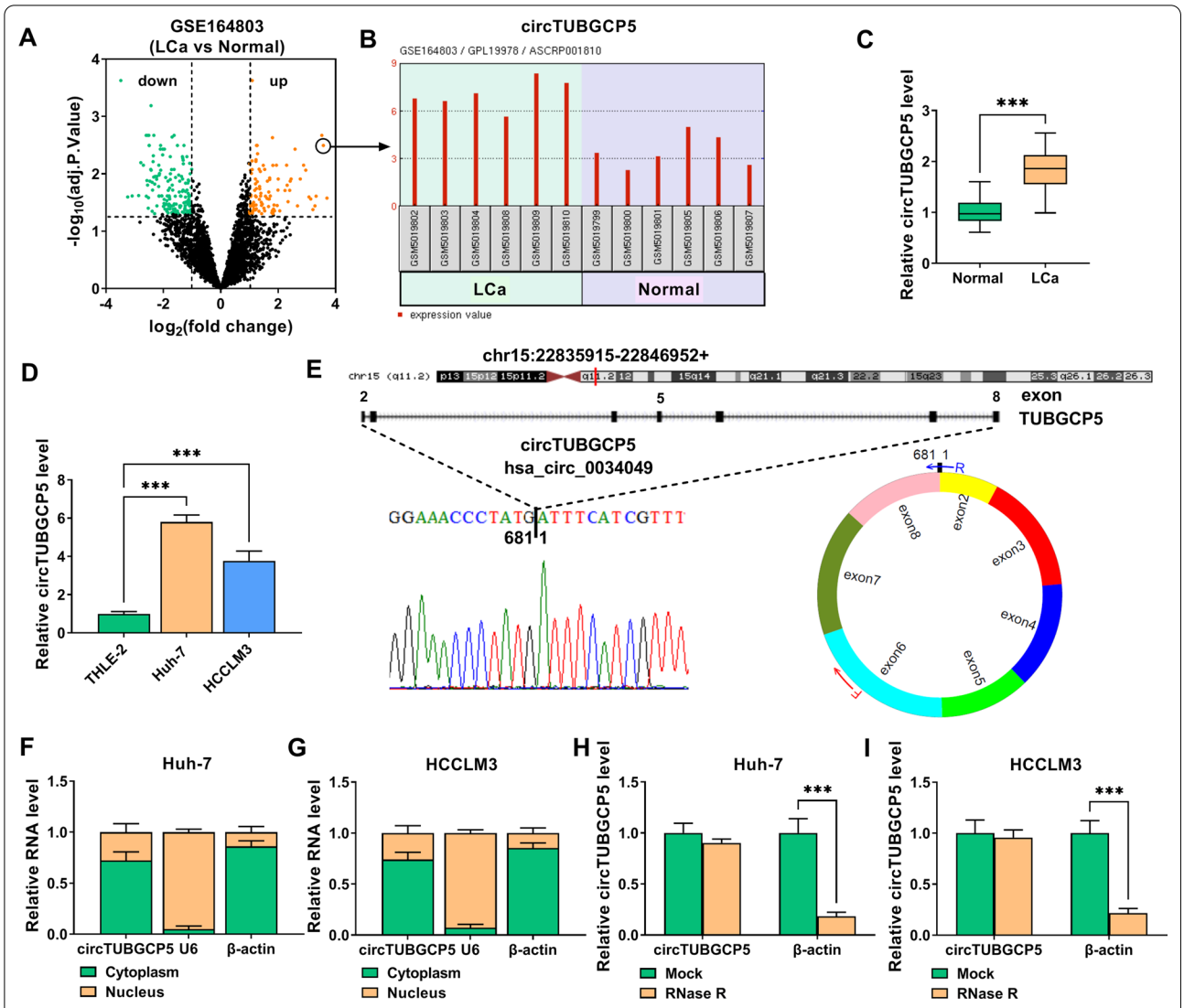

Fig. 1 CircTUBGCP5 was overexpressed in LCa tissues and cells. **A** Volcano plot of the differentially expressed circRNAs between LCa and normal samples in GSE164803 datasets. **B** The expression value of circTUBGCP5 in GSE164803 datasets. **C** The circTUBGCP5 level in LCa (n = 46) and normal (n = 46) tissues by qRT–PCR. **D** The circTUBGCP5 level in LCa cells (Huh-7 and HCCLM3) and normal cells (THLE-2) using qRT–PCR. **E** Scheme illustrated the production of circTUBGCP5. PCR primers used to specifically detect circTUBGCP5 by qRT–PCR were indicated by F (Forward primer) and R(Reward primer). The back-splice junction of circTUBGCP5 was identified by Sanger sequencing. **F** and **G** CircTUBGCP5 were abundant in the cytoplasm of Huh-7 and HCCLM3 cells, β-actin and U6 were applied as positive controls in the cytoplasm and nucleus, respectively. **H** and **I** qRT–PCR examined the RNA level of circTUBGCP5 and β-actin with RNase R treatment in Huh-7 and HCCLM3 cells. Data were expressed as mean ± SD. ***$P < 0.001$

gepia2.cancer-pku.cn/#index) [27] was analyzed to select the TOP 100 up-regulated genes in LCa (Dataset: Liver hepatocellular carcinoma (LIHC), Differential Methods: ANOVA, Differentially expressed genes: Log2FC > 1 and q-value < 0.01). Venn diagrams presented that ACSL4 was found as the putative target gene (Fig. 4A). Based on the GEPIA database, the results indicated that ACSL4 was up-regulated in the LIHC tumor than in normal tissues (Fig. 4B), and high expression of ACSL4 was negatively associated with the overall survival of LCa patients (Fig. 4C). ACSL4 mRNA and protein expression levels were up-regulated in LCa tissues than normal tissues (Fig. 4D, E). Additionally, the ACSL4 protein level was significantly increased in LCa cells (Fig. 4F). There were two complementary base sequences between ACSL4 3'UTR (position 1355–1360 and position 1380–1385) and miR-144-3p (Fig. 4G). Surprisingly, the results of the luciferase reporter assays showed that

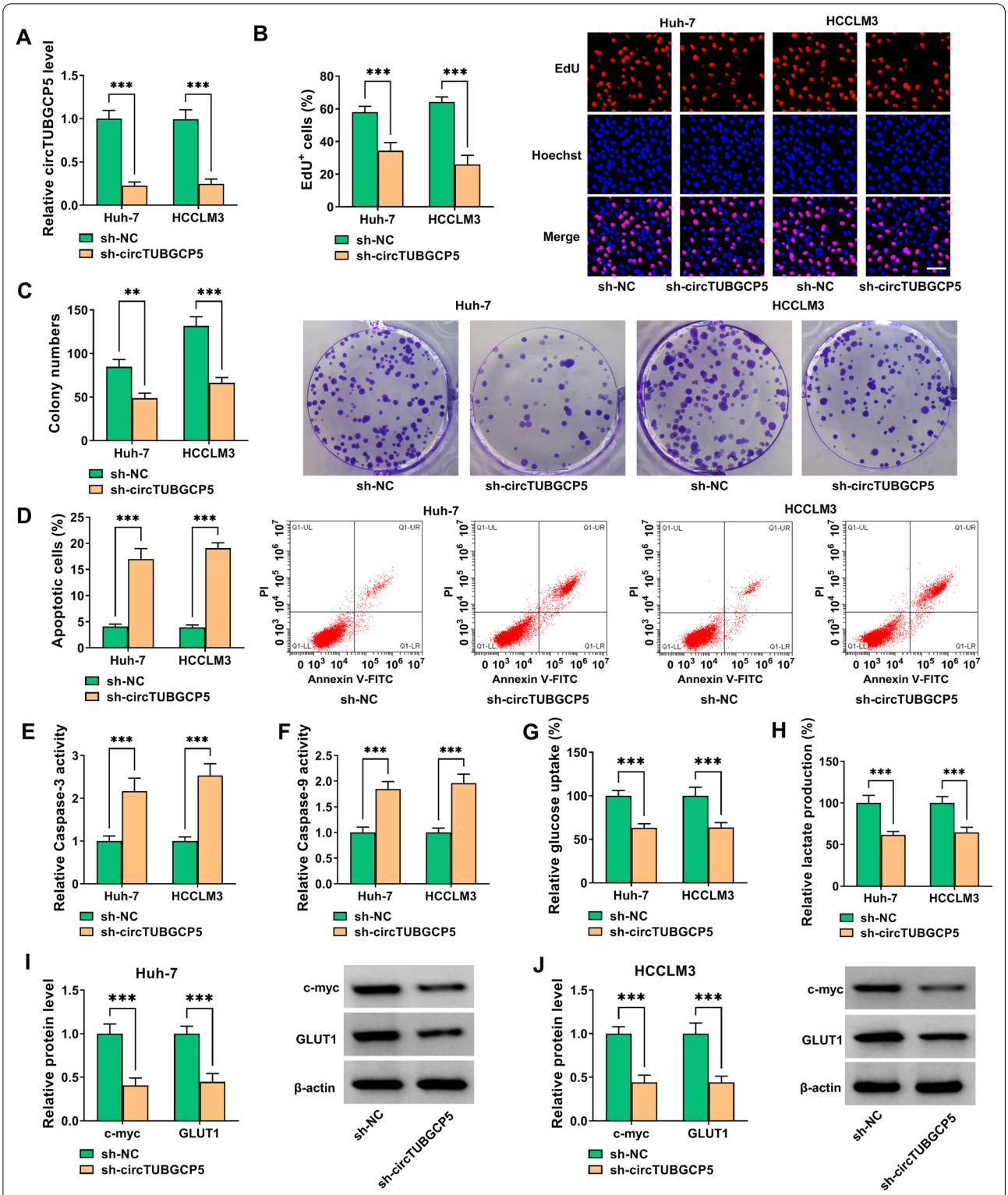

Fig. 2 circTUBGCP5 enhanced LCa cell proliferation, anti-apoptotic ability, and glycolysis. **A** The circTUBGCP5 level after transfecting the pLKO.1-puro-sh-NC (sh-NC) vector and pLKO.1-puro-sh-circTUBGCP5 (sh-circTUBGCP5) vector by qRT–PCR. **B** EdU assay, the scale bar represents 50 μm, **C** colony formation assay, **D** Annexin V-FITC/PI assay following knockdown of circTUBGCP5. **E** Caspase-3 activity, **F** Caspase-9 activity, **G** glucose uptake, and **H** lactate production in transfected with sh-NC or sh-circTUBGCP5 of Huh-7 and HCCLM3 cells. **I** and **J** The protein level of c-myc and GLUT1 by western blot assay. Data were expressed as mean ± SD. $^{**}P < 0.01$, $^{***}P < 0.001$

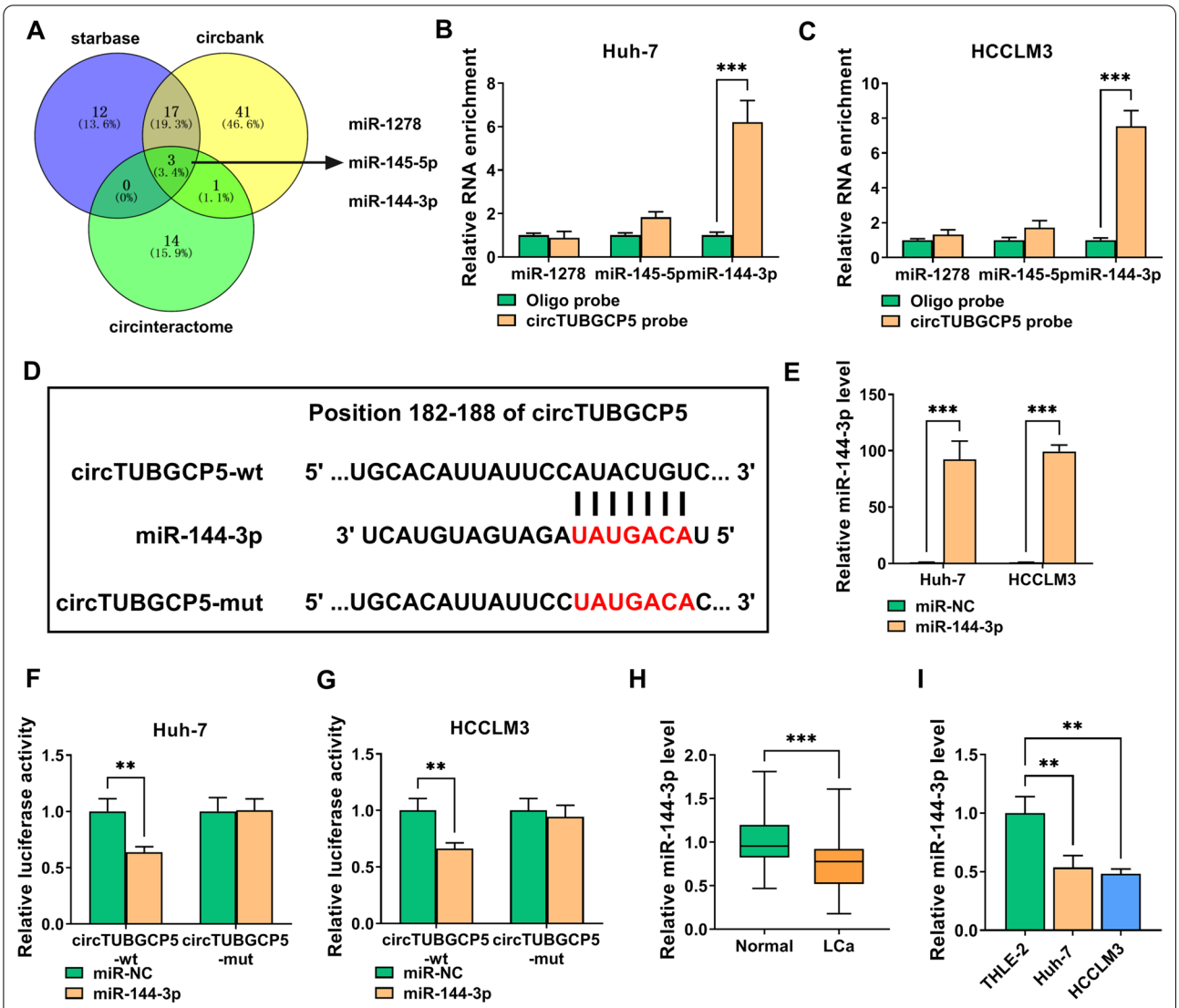

Fig. 3 CircTUBGCP5 may act as a sponge for miR-144-3p. **A** MiR-1278, miR-145-5p, and miR-144-3p were identified to possibly interact with circTUBGCP5 through the intersection of circintractome, starbase, and circbank databases. **B** and **C** The interaction of circTUBGCP5 and miR-144-3p was identified by RNA-pull down assay. **D** The schematic drawing showed the sequence of wild-type (wt) and mutant (mut) circTUBGCP5. **E** Overexpression efficiency of miR-144-3p using qRT–PCR. **F** and **G** The luciferase activity of circTUBGCP5-wt and circTUBGCP5-mut in Huh-7 and HCCLM3 cells after cotransfection with miR-144-3p. **H** The miR-144-3p level in LCa (n = 46) and normal (n = 46) tissues by qRT–PCR. **I** The circTUBGCP5 level in LCa cells (Huh-7 and HCCLM3) and normal cell (THLE-2) using qRT–PCR. Data were presented as mean ± SD. $^{**}P < 0.01$, $^{***}P < 0.001$

miR-144-3p significantly reduced the luciferase activity of the reporter ACSL4 3′UTR-wt compared to that of the reporter (1355–1360)-mut and (1380–1385)-mut of ACSL4 3′UTR (Fig. 4H, I). To measure if miR-144-3p regulated the expression of ACSL4 in LCa, miR-144-3p inhibitor (anti-miR-144-3p) was transfected into Huh-7 and HCCLM3 cells (Fig. 4J). Further, the western blot assay indicated that miR-144-3p inhibited ACSL4 expression and whether anti-miR-144-3p promoted ACSL4 expression in Huh-7 and HCCLM3 cells (Fig. 4K, L).

MiR-144-3p modulated LCa cell proliferation, anti-apoptotic ability, and glycolysis via targeting ACSL4

To investigate the effect of miR-144-3p and ACSL4 on LCa development, the overexpression efficiency of ACSL4 was verified by qRT–PCR (Fig. 5A). Functionally, as revealed by EdU (Fig. 5B), colony formation (Fig. 5C), and Annexin V-FITC/PI (Fig. 5D–F) assays, miR-144-3p could inhibit the proliferation and anti-apoptotic ability of Huh-7 and HCCLM3 cells, while the suppression could be blocked by overexpression of

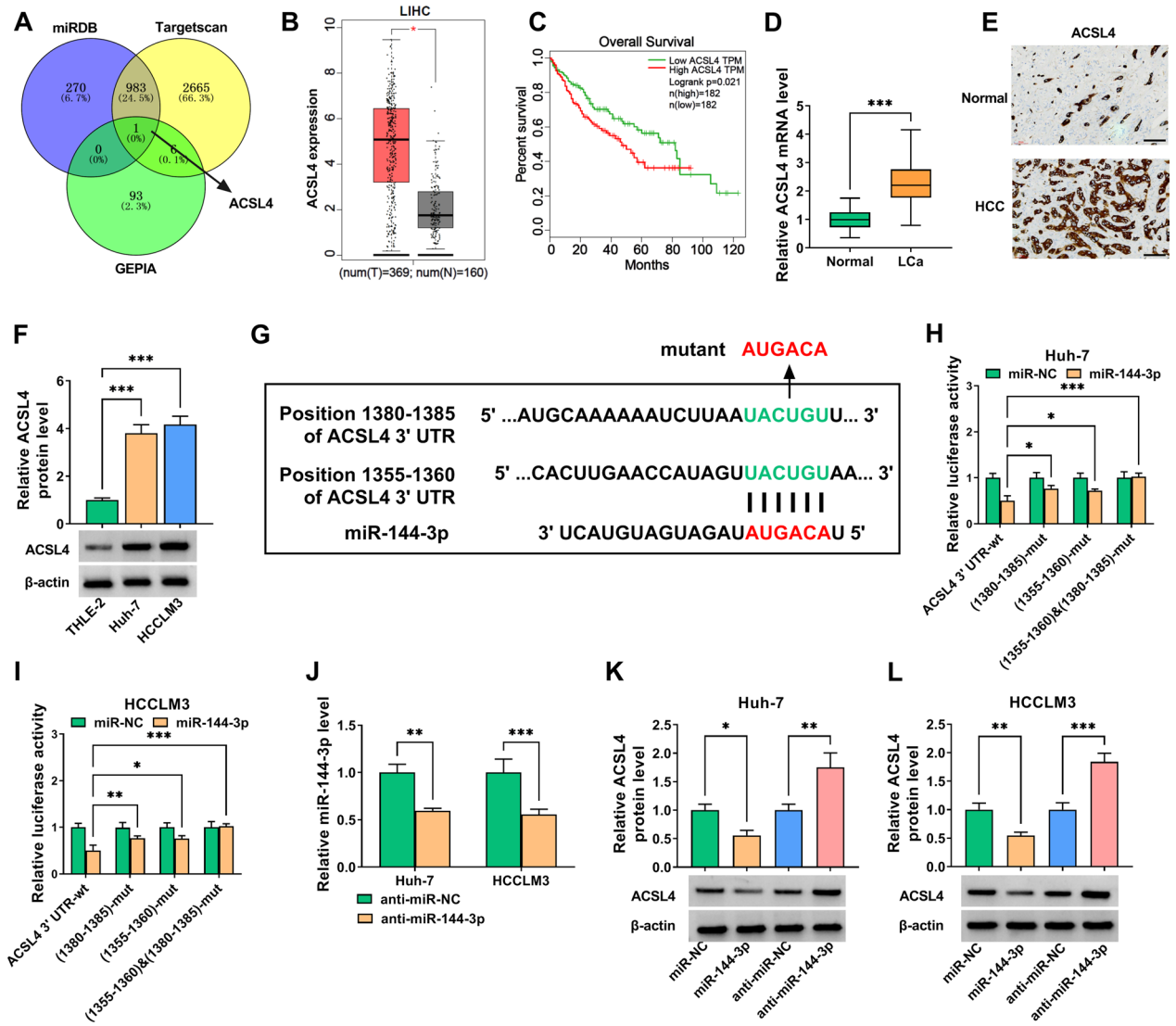

Fig. 4 MiR-144-3p targeted ACSL4 in LCa cells. **A** ACSL4 was identified to possibly interact with miR-144-3p and LCa by the intersection of Targetscan, miRDB, and GEPIA databases. **B** The expression of ACSL4 in LIHC tumor (n = 370) and normal (n = 50) in GEPIA database. **C** Overall survival (OS) analysis in LIHC based on ACSL4 expression in the GEPIA database. **D** The ACSL4 mRNA level in LCa (n = 46) and normal (n = 46) tissues by qRT–PCR. **E** IHC analysis of ACSL4 expression in LCa and normal tissues, the scale bar represents 100 μm. **F** The ACSL4 protein level in LCa cells (Huh-7 and HCCLM3) and normal cells (THLE-2) using western blot. **G** Schematic drawing showed the sequence of wild-type (wt) and mutant (mut) ACSL4 3′UTR. **H** and **I** The direct binding between ACSL4 3′UTR and miR-144-3p was analyzed by dual-luciferase reporter assay. **J** The miR-144-3p level in Huh-7 and HCCLM3 cells after transfection with anti-miR-144-3p or anti-miR-NC. **K** and **L** Western blot assay analyzed the ACSL4 expression in miR-144-3p inhibition and overexpressed Huh-7 and HCCLM3 cells. Data were presented as mean ± SD. *$P < 0.05$, **$P < 0.01$, ***$P < 0.001$

ACSL4. The decrease in cell glucose uptake and lactate production, which was induced by miR-144-3p overexpression, was reversed following ACSL4 upregulation in Huh-7 and HCCLM3 cells (Fig. 5G, H). Similarly, ACSL4 effectively abrogated the inhibited level of ACSL4, c-myc, and GLUT1 induced by miR-144-3p in Huh-7 and HCCLM3 cells (Fig. 5I, J). In summary, miR-144-3p may blunt LCa progression and glycolysis via targeting ACSL4.

CircTUBGCP5 promoted the malignant behaviors and glycolysis in LCa cells through the miR-144-3p/ACSL4 axis

To demonstrate if circTUBGCP5 contributed to the malignant behaviors and glycolysis by sponging miR144-3p, and then up-regulating ACSL4 expression, Huh-7 and HCCLM3 cells were transfected with sh-NC + anti-miR-NC + pcDNA, sh-circTUBGCP5 + anti-miR-NC + pcDNA,

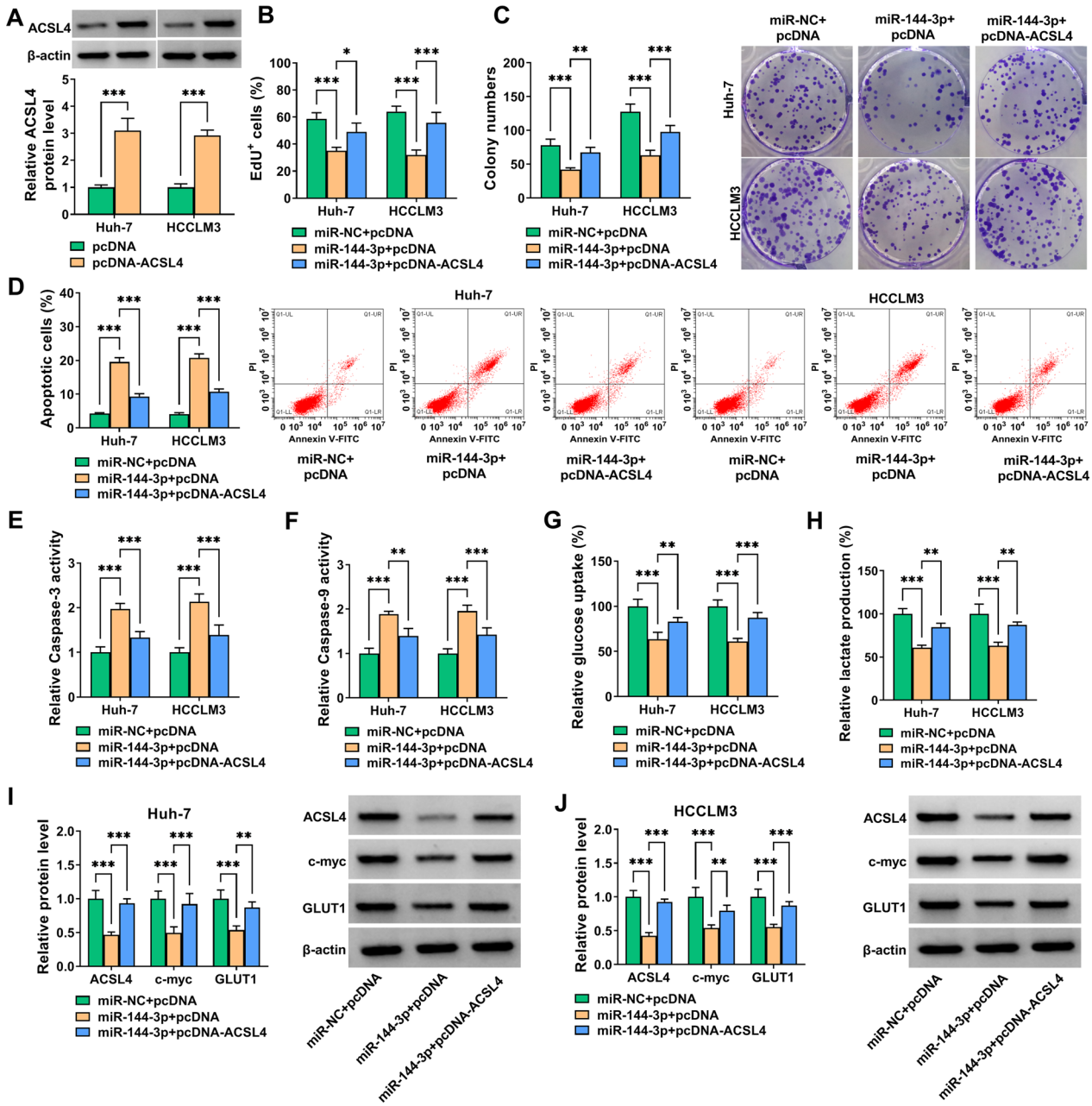

Fig. 5 ACSL4 reversed the function of miR-144-3p in LCa. **A** Transfection efficacy of ACSL4 overexpression was validated in Huh-7 and HCCLM3 cells via western blot. **B** and **C** Cell proliferation, **D** apoptosis, **E** Caspase-3 activity, **F** Caspase-9 activity, **G** glucose uptake, **H** lactate production, **I** and **J** ACSL4, c-myc, and GLUT1 protein level were detected in Huh-7 and HCCLM3 cells after overexpressing miR-144-3p in the presence or absence of pcDNA-ACSL4. Data were expressed as mean ± SD. *$P < 0.05$, **$P < 0.01$, ***$P < 0.001$

sh-circTUBGCP5 + anti-miR-144-3p + pcDNA, or sh-circTUBGCP5 + anti-miR-NC + pcDNA-ACSL4. The effects of sh-circTUBGCP5 on proliferation (Fig. 6A, B), anti-apoptotic ability (Fig. 6C–E), and glycolysis (Fig. 6F, G) were counteracted by miR-144-3p down-regulation or ACSL4 up-regulation in Huh-7 and HCCLM3 cells. The sh-circTUBGCP5 led to inhibition of the cell glucose uptake and lactate production capabilities, but these effects could be partially attenuated by the anti-miR-144-3p or the pcDNA-ACSL4 up-regulation. In addition, inhibition of miR-144-3p or ectopic ACSL4 expression reversed the inhibitory effect of sh-circTUBGCP5 on the expression of ACSL4, c-myc, and

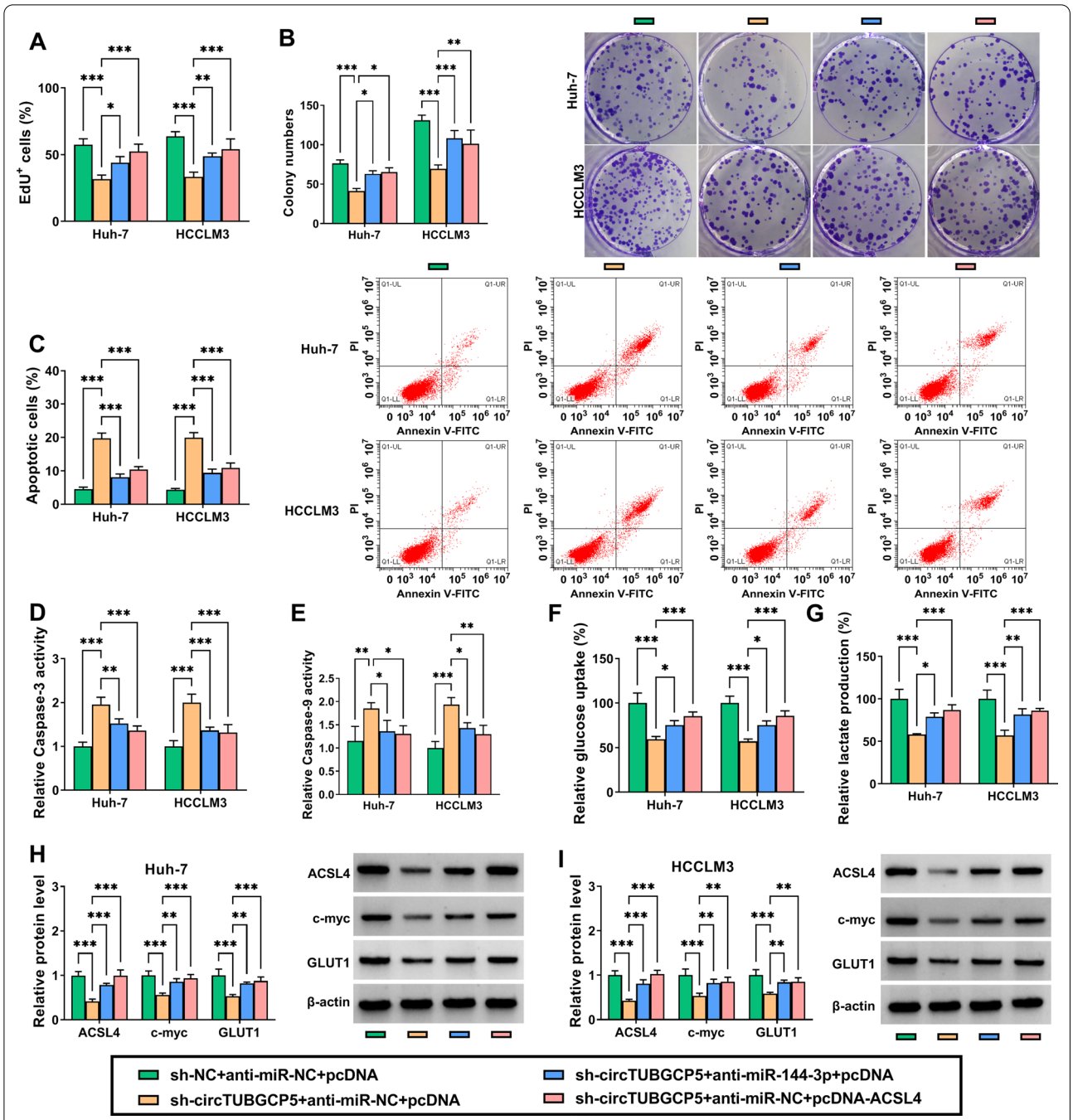

Fig. 6 CircTUBGCP5 promoted the malignant behaviors and glycolysis in LCa cells through the miR-144-3p/ACSL4 axis. **A** and **B** Cell proliferation, **C** apoptosis, **D** Caspase-3 activity, **E** Caspase-9 activity, **F** glucose uptake, **G** lactate production, **H** and **I** ACSL4, c-myc, and GLUT1 protein level in Huh-7 and HCCLM3 cells after silencing circTUBGCP5 in the presence or absence of anti-miR-144-3p or pcDNA-ACSL4. Data were expressed as mean ± SD. *$P < 0.05$, **$P < 0.01$, ***$P < 0.001$

GLUT1 in Huh-7 and HCCLM3 cells (Fig. 6H, I). These results indicated that circTUBGCP5 may enhance the proliferation, anti-apoptotic ability, and glycolysis in LCa cells through the miR-144-3p/ACSL4 axis.

CircTUBGCP5 boosted LCa tumor growth in vivo

To further examine the ability of circTUBGCP5 LCa growth in vivo, we generated xenografts in nude mice. circTUBGCP5 down-regulation remarkably hindered the tumor volumes and weights (Fig. 7A, B). circTUBGCP5

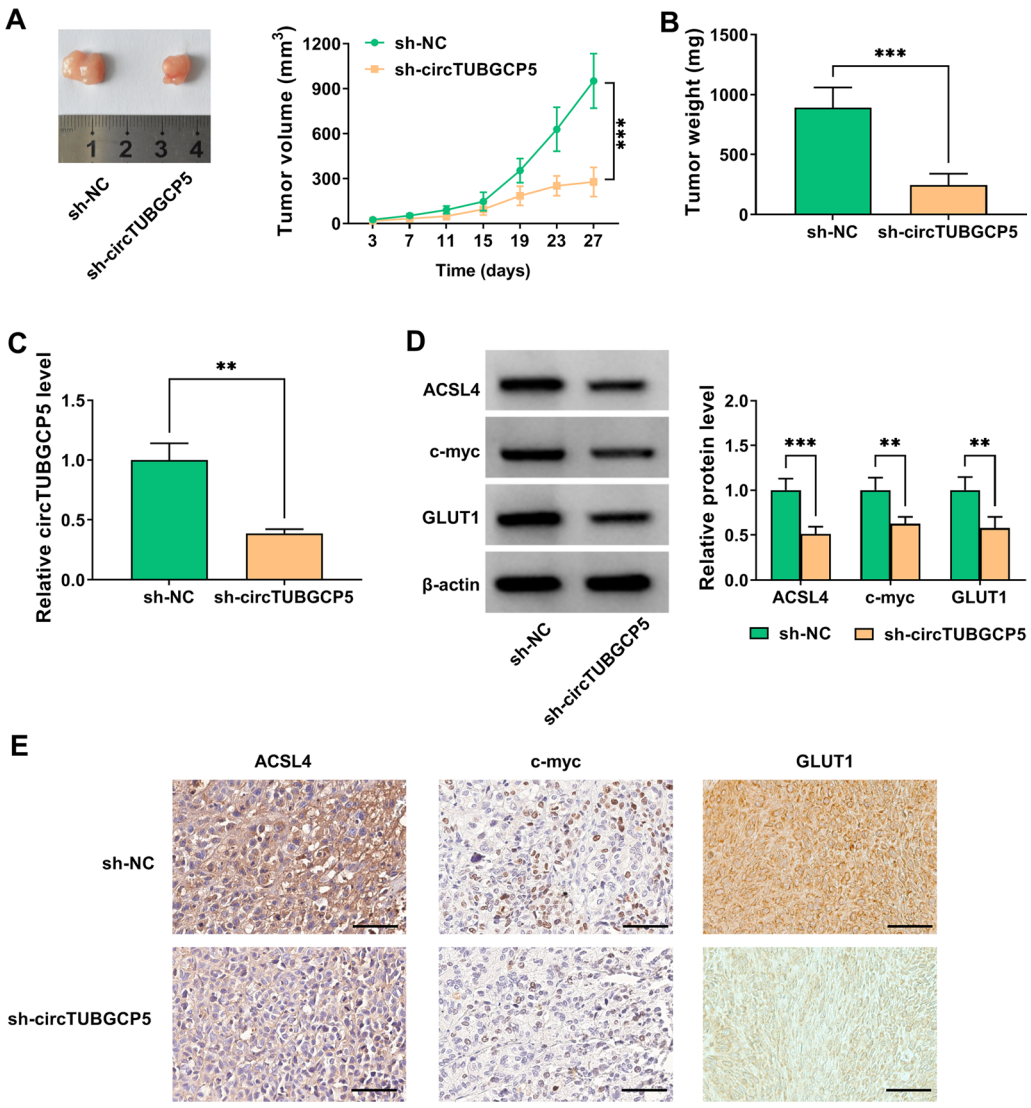

Fig. 7 CircTUBGCP5 enhanced LCa tumor growth in vivo. **A** Tumor volume and **B** tumor weight were monitored in the sh-NC group (n = 5) and sh-circTUBGCP5 group (n = 5). **C** qRT–PCR analysis of the circTUBGCP5 level. **D** Western blot and **E** IHC analysis of the ACSL4, c-myc, and GLUT1 protein levels in different group xenografts, the scale bar represents 100 μm. Data were shown as mean ± SD. $^{**}P < 0.01$, $^{***}P < 0.001$

level was significantly reduced in the tumor tissue of the sh-circTUBGCP5 group than in the sh-NC group (Fig. 7C). Additionally, western blot (Fig. 7D) and IHC (Fig. 7E) data uncovered that circTUBGCP5 down-regulation weakened the protein level of ACSL4, c-myc, and GLUT1 in tumor tissue. Collectively, these results manifested that circTUBGCP5 regulated ACSL4 expression to promote LCa growth in vivo.

Discussion

Currently, we identified a novel circRNA named circTUBGCP5, which was also much higher in LCa tissues and cells. To our knowledge, this work is the first study to explore the expression and function of circTUBGCP5 in LCa. Furthermore, the circTUBGCP5/miR-144-3p/ACSL4 axis is also discovered at first in LCa.

In recent years, a massive number of evidences have implicated that metabolic reprogramming was closely related to the occurrence and development of LCa, in which glycolysis was one of the most prominent features, but its mechanism was not fully understood. Until recently, a small amount of studies showed circRNA may provide new insight into the glycolysis of LCa. For instance, CircC16or62 contributed to malignancy and glycolysis via sponging miR-138-5p to increase the protein kinase PTK2 level in LCa [28]. Up-regulated

hsa_circ_0016788 could enhance hepatocellular carcinoma cell glycolysis, invasion, and growth, whereas inhibiting cell apoptosis via the miR-506-3p/PARP14 pathway [29]. However, the effect of circTUBGCP5 on LCa glycolysis remained largely unknown. Furthermore, knockdown of endogenous circTUBGCP5 in Huh-7 and HCCLM3 cells effectively constrained proliferation, anti-apoptotic ability, glucose uptake, lactate production, and tumor growth in vivo. We further found that circTUBGCP5 could promote protein expression of c-myc, a key regulator of glycolysis in tumor cells, and GLUT1, one of the most important glycolytic transporters in the glycolytic pathway. These observations showed that circTUBGCP5 could induce LCa glycolysis by boosting c-myc and GLUT1 expression.

The mechanism of circRNA in tumorigenesis and progression has not been elucidated. The most widely reported function of circRNA is to act as a miRNA sponge in the cell cytoplasm [7, 9]. In this research, we screened three miRNAs and further confirmed that miR-144-3p could bind to circTUBGCP5 by RNA pull-down assay and dual-luciferase reporter assay. Then, we filtered out one gene predicted to exert cancer-promoting effects and demonstrated that miR-144-3p was capable of binding to ACSL4 3′UTR. miR-144-3p, which was involved in glucose metabolism in colon cancer cells [30], was down-regulated in extensive human cancers including LCa [31]. For example, miR-144-3p hindered cell growth, invasion, and M1 polarization of tumor-associated macrophages via targeting EIF4G2 [32], DOCK4 [33], EZH2 [34], and HGF [34] in LCa. ACSL4, a key enzyme of fat metabolism in the body, has been manifested as an oncogene to be associated with many malignant tumors, such as prostate cancer [35], breast cancer [36], and LCa [37–40]. It was previously uncovered that ACSL4 could stabilize c-myc [40] and GLUT1 [37] protein by reducing their ubiquitination to facilitate LCa progression. Consistent with previous research outcomes, miR-144-3p was down-regulated but ACSL4 was up-regulated in LCa tissues and cells versus normal tissues and cells. Kaplan–Meier analysis also uncovered that high expression of ACSL4 was negatively associated with the overall survival of LCa patients. Exhilaratingly, miR-144-3p could impede LCa progression via targeting ACSL4. As expected, c-myc and GLUT1 mediated the circTUBGCP5/miR-144-3p/ACSL4-induced promotional effect on LCa proliferation, anti-apoptotic ability, and glycolysis. However, whether ubiquitination of c-myc and GLUT1 can be modulated by the circTUBGCP5/miR-144-3p/ACSL4 axis need further study.

This work has several limitations. First, our study revealed that circTUBGCP5 expression was significantly up-regulated in 46 pairs LCa tissues. Further investigation of circTUBGCP5 in clinical significance by recruiting more LCa patients. Second, due to the limitation of time, we did not study the association between the circTUBGCP5/miR-144-3p/ACSL4 axis and LCa patient survival. Third, circTUBGCP5 may employ as a sponge for protein or encoding peptides to regulate the development of LCa, which will be an important question for our future investigation.

Ultimately, we reported circTUBGCP5 was increased in LCa and characterized the facilitation that circTUBGCP5 played on the expression of c-myc and GLUT1 via miR-144-3p/ACSL4 axis to enhance proliferation, anti-apoptotic ability, and glycolysis, which in turn contributed to LCa progression. Taken together, circTUBGCP5/miR-144-3p/ACSL4 axis may be used as a diagnostic biomarker and potential target in LCa therapy.

Acknowledgements
None.

Author contributions
WD conducted the experiments and drafted the manuscript, designed and supervised the study. WY collected and analyzed the data. YD contributed the methodology. SW operated the software and edited the manuscript. All the authors read and approved the final manuscript.

Funding
None.

Availability of data and materials
The data sets used and/or analyzed during the current study are available from the corresponding author on reasonable request.

Declarations

Competing interests
The authors declare that they have no conflicts of interest.

Author details
[1]Hepatopancreatobiliary Surgery, The First Affiliated Hospital of Anhui Medical University, No.218 Jixi Road, Hefei 230022, Anhui, People's Republic of China. [2]Dermatology Department, The First Affiliated Hospital of Anhui Medical University, Hefei, Anhui, China.

Received: 17 May 2022 Accepted: 28 July 2022
Published online: 20 August 2022

References

1. Sung H, Ferlay J, Siegel RL et al (2021) Global cancer statistics 2020: GLOBOCAN estimates of incidence and mortality worldwide for 36 cancers in 185 countries. CA Cancer J Clin 71(3):209–249
2. Feng J, Li J, Wu L et al (2020) Emerging roles and the regulation of aerobic glycolysis in hepatocellular carcinoma. J Exp Clin Cancer Res 39(1):126
3. Yang JD, Hainaut P, Gores GJ, Amadou A, Plymoth A, Roberts LR (2019) A global view of hepatocellular carcinoma: trends, risk, prevention and management. Nat Rev Gastroenterol Hepatol 16(10):589–604
4. Villanueva A (2019) Hepatocellular carcinoma. N Engl J Med 380(15):1450–1462
5. Kosvyra A, Maramis C, Chouvarda I (2019) Developing an integrated genomic profile for cancer patients with the use of NGS data. Emerg Sci J 3:157–167
6. Elalfy M, Borlak J (2021) Exon array analysis to identify diethyl-nitrosamine differentially regulated and alternately spliced genes in early liver

carcinogenesis in the transgenic mouse ATT-myc model. Sci Med J 3:2704–9833
7. Ebbesen K, Kjems J, Hansen T (2016) Circular RNAs: identification, biogenesis and function. Biochim Biophys Acta. 1859(1):163–168
8. Han B, Chao J, Yao H (2018) Circular RNA and its mechanisms in disease: from the bench to the clinic. Pharmacol Ther. 187:31–44
9. Hansen T, Jensen T, Clausen B et al (2013) Natural RNA circles function as efficient microRNA sponges. Nature 495(7441):384–388
10. Tao M, Zheng M, Xu Y, Ma S, Zhang W, Ju S (2021) CircRNAs and their regulatory roles in cancers. Mol Med 27(1):94
11. Li T, Xian HC, Dai L, Tang YL, Liang XH (2021) Tip of the iceberg: roles of CircRNAs in cancer glycolysis. OncoTargets Ther. 14:2379–2395
12. Guan H, Luo W, Liu Y, Li M (2021) Novel circular RNA circSLIT2 facilitates the aerobic glycolysis of pancreatic ductal adenocarcinoma via miR-510-5p/c-Myc/LDHA axis. Cell Death Dis 12(7):645
13. Mo Y, Wang Y, Zhang S et al (2021) Circular RNA circRNF13 inhibits proliferation and metastasis of nasopharyngeal carcinoma via SUMO2. Mol Cancer 20(1):112
14. Chen J, Wu Y, Luo X et al (2021) Circular RNA circRHOBTB3 represses metastasis by regulating the HuR-mediated mRNA stability of PTBP1 in colorectal cancer. Theranostics 11(15):7507–7526
15. Pavlova N, Thompson C (2016) The emerging hallmarks of cancer metabolism. Cell Metab 23(1):27–47
16. El Hassouni B, Granchi C, Vallés-Martí A et al (2020) The dichotomous role of the glycolytic metabolism pathway in cancer metastasis: interplay with the complex tumor microenvironment and novel therapeutic strategies. Semin Cancer Biol 60:238–248
17. Kim J, DeBerardinis R (2019) Mechanisms and implications of metabolic heterogeneity in cancer. Cell Metab 30(3):434–446
18. Jiang Y, Han Q, Zhao H, Zhang J (2021) Promotion of epithelial-mesenchymal transformation by hepatocellular carcinoma-educated macrophages through Wnt2b/β-catenin/c-Myc signaling and reprogramming glycolysis. J Exp Clin Cancer Res 40(1):13–13
19. Shang R, Wang M, Dai B et al (2020) Long noncoding RNA SLC2A1-AS1 regulates aerobic glycolysis and progression in hepatocellular carcinoma via inhibiting the STAT3/FOXM1/GLUT1 pathway. Mol Oncol 14(6):1381–1396
20. Yu L, Kim J, Jiang L et al (2020) MTR4 drives liver tumorigenesis by promoting cancer metabolic switch through alternative splicing. Nat Commun 11(1):708–708
21. Zhong S, Wang J, Zhang Q, Xu H, Feng J (2018) CircPrimer: a software for annotating circRNAs and determining the specificity of circRNA primers. BMC Bioinformatics 19(1):292
22. Li JH, Liu S, Zhou H, Qu LH, Yang JH (2014) starBase v2.0: decoding miRNA-ceRNA, miRNA-ncRNA and protein-RNA interaction networks from large-scale CLIP-Seq data. Nucleic Acids Res. 42(D1):D92-97
23. Liu M, Wang Q, Shen J, Yang BB, Ding X (2019) Circbank: a comprehensive database for circRNA with standard nomenclature. RNA Biol 16(7):899–905
24. Dudekula D, Panda A, Grammatikakis I, De S, Abdelmohsen K, Gorospe M (2016) CircInteractome: a web tool for exploring circular RNAs and their interacting proteins and microRNAs. RNA Biol 13(1):34–42
25. Chen Y, Wang X (2020) miRDB: an online database for prediction of functional microRNA targets. Nucleic Acids Res 48(D1):D127–D131
26. Agarwal V, Bell GW, Nam J-W, Bartel DP (2015) Predicting effective microRNA target sites in mammalian mRNAs. Elife 4:e05005
27. Tang Z, Li C, Kang B, Gao G, Li C, Zhang Z (2017) GEPIA: a web server for cancer and normal gene expression profiling and interactive analyses. Nucleic Acids Res 45(W1):W98–W102
28. Zhang S, Lu Y, Jiang HY et al (2021) CircC16orf62 promotes hepatocellular carcinoma progression through the miR-138-5p/PTK2/AKT axis. Cell Death Dis 12(6):597–597
29. Chen M, Hu G, Zhou X, Peng Z, Wen W (2021) Hsa_circ_0016788 regulates glycolysis and proliferation via miR-506-3p/PARP14 axis of hepatocellular carcinoma. J Gastroenterol Hepatol 36(12):3457–3468
30. Cui Z, Wang Q, Deng M, Han Q (2022) LncRNA HCG11 promotes 5-FU resistance of colon cancer cells through reprogramming glucose metabolism by targeting the miR-144-3p-PDK4 axis. Cancer Biomark 34(1):41–53
31. Kooshkaki O, Rezaei Z, Rahmati M et al (2020) MiR-144: a new possible therapeutic target and diagnostic/prognostic tool in cancers. Int J Mol Sci 21(7):2578
32. Li S, Shao J, Lou G, Wu C, Liu Y, Zheng M (2021) MiR-144-3p-mediated dysregulation of EIF4G2 contributes to the development of hepatocellular carcinoma through the ERK pathway. J Exp Clin Cancer Res 40(1):53
33. Li H, Wang M, Zhou H, Lu S, Zhang B (2020) EBLN3P long noncoding RNA promotes the progression of liver cancer via alteration of microRNA-144-3p/DOCK4 signal. Cancer Manag Res 12:9339–9349
34. Zhao J, Li H, Zhao S et al (2021) Epigenetic silencing of miR-144/451a cluster contributes to HCC progression via paracrine HGF/MIF-mediated TAM remodeling. Mol Cancer 20(1):46
35. Jiang X, Guo S, Zhang Y et al (2020) LncRNA NEAT1 promotes docetaxel resistance in prostate cancer by regulating ACSL4 via sponging miR-34a-5p and miR-204-5p. Cell Signal 65:109422
36. Wang H, Xu B, Zhang X, Zheng Y, Zhao Y, Chang X (2016) PADI2 gene confers susceptibility to breast cancer and plays tumorigenic role via ACSL4, BINC3 and CA9 signaling. Cancer Cell Int 16:61
37. Wang J, Wang Z, Yuan J, Wang J, Shen X (2020) The positive feedback between ACSL4 expression and O-GlcNAcylation contributes to the growth and survival of hepatocellular carcinoma. Aging 12(9):7786–7800
38. Qin X, Zhang J, Lin Y, Sun X, Zhang J, Cheng Z (2020) Identification of MiR-211-5p as a tumor suppressor by targeting ACSL4 in hepatocellular carcinoma. J Transl Med 18(1):326
39. Chen J, Ding C, Chen Y et al (2021) ACSL4 reprograms fatty acid metabolism in hepatocellular carcinoma via c-Myc/SREBP1 pathway. Cancer Lett 502:154–165
40. Chen J, Ding C, Chen Y et al (2020) ACSL4 promotes hepatocellular carcinoma progression via c-Myc stability mediated by ERK/FBW7/c-Myc axis. Oncogenesis 9(4):42

Publisher's Note

Springer Nature remains neutral with regard to jurisdictional claims in published maps and institutional affiliations.

Submit your manuscript to a SpringerOpen journal and benefit from:

- ► Convenient online submission
- ► Rigorous peer review
- ► Open access: articles freely available online
- ► High visibility within the field
- ► Retaining the copyright to your article

Submit your next manuscript at ► springeropen.com